

# Petrography and geochemistry of volcanic rocks in the Khao Sam Sip, Sa Kaeo, Eastern Thailand

Maythira Sriwichai<sup>1\*</sup>, Abhisit Salam<sup>1</sup>, Takayuki Manaka<sup>2</sup>

<sup>1</sup>*Department of Geology, Faculty of Science, Chulalongkorn University, Bangkok 10330, Thailand*

<sup>2</sup>*Mineral Resources Research Group, Research Institute for Geo-Resources and Environment, Geological Survey of Japan (AIST), Tsukuba, Ibaraki 305-8567, Japan*

\*Corresponding author e-mail: maythira.saw@gmail.com

## Abstract

The volcanic rocks at Khao Sam Sip, Sa Kaeo province is a part of the Loei-Phetchabun-Sa Kaeo Volcanic Belt. Based on field observation, petrographic and geochemical studies, the rocks in the study area can be divided into four rock units namely, 1) Coherent volcanic unit, 2) Intermediate-mafic breccia unit, 3) Volcanogenic-sedimentary unit, 4) Sedimentary unit. Unit 1 is the lowest unit in the sequence consisting of olivine-pyroxene-plagioclase basalt, pyroxene-phyric basalt, hornblende-plagioclase andesite, and plagioclase-phyric andesite. Unit 2 consists of polymictic andesitic breccia and polymictic andesitic sandstone. Unit 3 involves volcanogenic sedimentary rocks comprising of crystal-lithic sandstone and polymictic conglomerate. Unit 4 is a sedimentary unit that includes fine-grained clastic rock and limestone. In the geochemical study, representative rock types mainly from the coherent volcanic unit were selected for geochemical analyzes including major, trace, and rare earth elements. They are ranged in compositions of trachyandesite and alkali basalt with few rhyodacite, andesite and basanite and classified dominantly as alkaline affinity. Based on the results of trace elements and REE abundances, the rocks can be subdivided into four groups. All of the four groups have similar chemical characters of enrichment in HFSE and light rare earth elements (LREE) with distinct negative Eu anomalies, and this may suggest that the rocks were formed from Early Triassic fractionated magma of volcanic arc system as a part of Loei Fold Belt. Copper-rich veins/veinlets are hosted in coherent volcanic rocks and they may represent either skarn or epithermal style mineralization.

**Keywords:** Volcanic Rock, Alkaline, Sa Kaeo, Loei-Petchabun-Sa Kaeo Volcanic Belt, Petrography, Geochemistry, Copper veins/veinlets

## 1. Introduction

In Thailand, pre-Cenozoic volcanic and plutonic rocks are important host rocks for mineral deposits especially for epithermal and skarn deposits such as Chatree (epithermal gold-silver), Khao Phanom Pha (gold skarn), Khao Lek and Khao Thap Kwai (iron skarn) (Khin Zaw et al., 2009) (Figure 1).

Thailand and its adjacent areas are composed of two terranes namely, Shan-Thai terrane in the west and Indochina terrane in the east (Fig 1). Between these terranes, there are Sukhothai Fold Belt (SFB) located on the eastern edge of Shan-Thai terrane and Loei Fold Belt (LFB) on the western edge of Indochina

terrane, represented by volcano-plutonic rocks (Bunopas and Vella, 1983; Barr et al., 2000). During Middle Permian to Late Triassic, the continuous subduction of the Shan-Thai underneath the Indochina lead to the formation of volcanic and plutonic rocks of the LFB, which is separated from Sukhothai Fold Belt by the Nan-Uttaradit and Sa Kaeo sutures representing back-arc basins (Figure 1; Bunopas and Vella, 1983; Intasopa, 1993; Sone and Metcalfe, 2008; Metcalfe, 2009). Subsequently, the Shan-Thai terrane collided with the Indochina terrane during the Late Triassic (Singharajwarapan, 1994; Charusiri et al., 2002).

In Thailand, the volcanic rocks were formed in two major periods, 1) Permo-Triassic and 2) Cenozoic periods. The Permo-Triassic volcanic rocks are grouped into four major volcanic belts: 1) Chiang Rai–Chiang Mai Volcanic Belt, 2) Chiang Khong–Lampang–Tak Volcanic Belt, 3) Nan–Uttaradit suture and Sa Kaeo suture and 4) Loei–Phetchabun–Nakhon Nayok Volcanic Belt (Figure 1; Barr and Macdonald, 1978; Jungyusuk and Khositanont, 1992; Panjasawatwong et al., 2006; Kosuwan et al., 2017). The Chiang Rai–Chiang Mai Volcanic Belt mainly comprises mafic lava, hyaloclastite, and pillow breccia ranging in composition of tholeiite to transitional tholeiite and might have been erupted during the Carboniferous and Permian to Triassic periods (Barr and Macdonald, 1978; Barr et al., 1990). The Chiang Khong–Lampang–Tak Volcanic Belt shows a wide range of compositions from basaltic to rhyolitic rocks with calc-alkalic affinity. It consists of lava and pyroclastic rocks and they might have been erupted during the Permo-Triassic and Late Triassic to Early Jurassic (Jungyusuk and Khositanont, 1992; Barr et al., 2000). The volcanic rocks in the Nan–Uttaradit suture and Sa Kaeo suture zones occur in small amount ranging composition from tholeiite to calc-alkaline and ages from Carboniferous to Triassic (Barr et al., 1987; Panjasawatwong and Yaowanoiyothin, 1993). Major volcanics in the LFB are mainly derived from subduction-related magmas and dominated with calc-alkalic affinity (Jungyusuk and Khositanont, 1992; Khin Zaw et al., 2014) with subordinated amount of tholeiite especially at Phichit–Phetchabun area (Salam, 2013; Salam et al. 2014). Major volcanic rocks in the LFB can be grouped into three main periods: 1) Silurian to Early Carboniferous, 2) Middle Permian to Late Triassic, and 3) Cenozoic (Intasopa and Dunn, 1994; Qian et al., 2017).

The volcanic rocks at Khao Sam Sip study area in Sa Kaeo Province have been previously mapped by Department of Mineral Resources at scale of 1: 250,000 and was

explored for gold in 2011. However, no detailed study has been undertaken particularly for detailed petrography, geochemistry and mineralization. In this study, focuses have been given to field checking of the pre-existing map of Department of Mineral Resources complied by Polprasit et al. (1985) and detailed petrography and geochemistry of volcanic rocks (coherent rocks). Limited study was also given to mineralization as available drill cores are less mineralized.

## 2. Geological setting

The volcanic rocks of Khao Sam Sip area are a part of Loei–Phetchabun–Nakhon Nayok volcanic belt. Jungyusuk and Khositanont (1992) reported that the volcanic rocks have felsic to mafic compositions consisting mainly of lavas and its pyroclastic rocks associated with ultramafic intrusions and gold bearing quartz lodes.

The Khao Sam Sip area is mountainous areas in which the highest peak is Khao Sam Sip (344 mRL) and surrounded with intermountain basin. Based on an updated mapping during this study, the study area is made up of sedimentary rocks. The youngest rock type consists of limestone and fine- to medium-grained greywacke interbedded shale, and this is underlain by volcanic rocks which can be further subdivided into three volcanic rock units (Figure 2). The classification of volcanic rocks is based on McPhie et al. (1993). Major geological units in the Khao Sam Sip area are described from the bottom to top as given below.

### 2.1 Coherent volcanics (Unit 1)

The rocks of coherent volcanic unit are mainly found in the northeast of study area at Khao Moei Choi (Figure 2) and intersected in diamond drill holes. This coherent volcanic unit is the lowest part of the sequence consisting of olivine-pyroxene-plagioclase basalt, pyroxene-phyric basalt, hornblende-plagioclase andesite

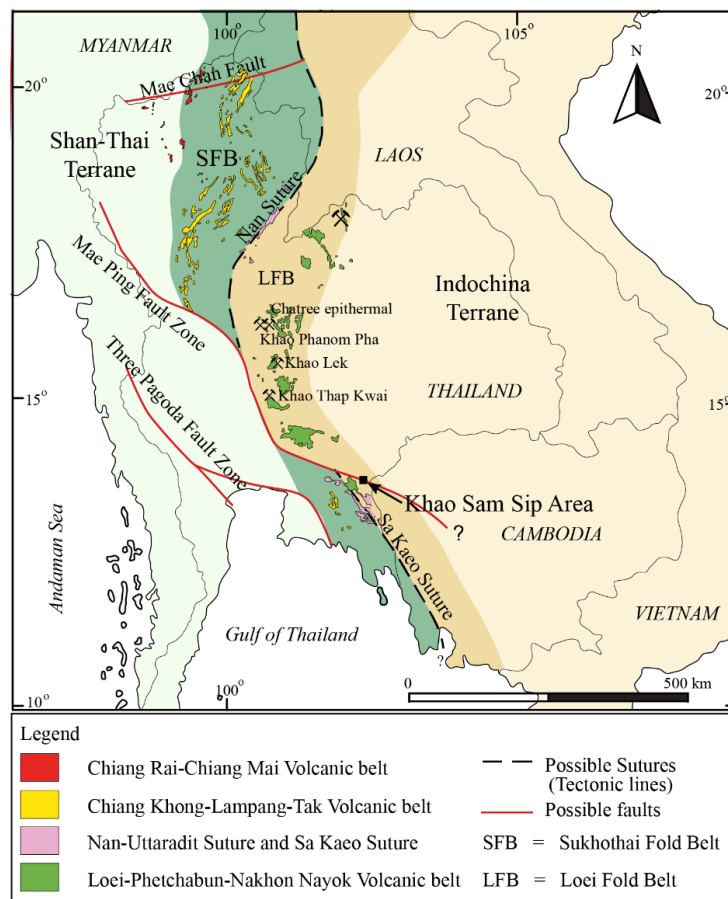


**Figure 1.** Tectonic map showing the major tectonic terranes and sutures (modified after Sone and Metcalfe, 2008; Morley, 2014) and distribution of Paleozoic-Mesozoic volcanic rocks in Thailand (after Jungyusuk and Khositanont, 1992; Panjasawatwong, 2006; Kosuwan et al., 2017)

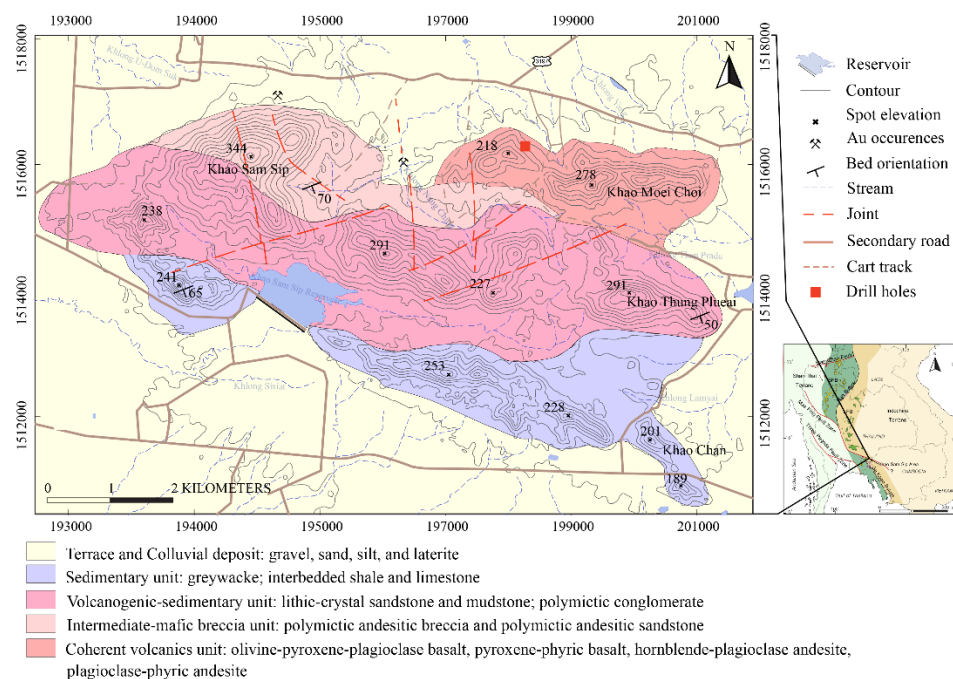


**Figure 2.** Geological map of the Khao Sam Sip area.

and plagioclase-phyric andesite. The outcrops of olivine-pyroxene-plagioclase basalt are found at the wall of small quarry located at the north of Khao Moei Choi (Figure 3A). This rock is characterized by porphyritic texture in which mafic phenocrysts include olivine, and pyroxene with some plagioclase phenocrysts (Figure 3B). The mafic phenocrysts are mainly  $<0.5$  mm size of olivine and clinopyroxene (Figure 3C). The Plagioclase phenocrysts are partly altered to sericite. The outcrop of pyroxene-phyric basalt has been found at the quarry located at the north of Khao Moei Choi and crosscut olivine-pyroxene-plagioclase basalt. This rock displays porphyritic texture with pyroxene and plagioclase phenocrysts. (Figure 3D). Under microscope, the pyroxene-phyric basalt is characterized by porphyritic texture with mainly  $>0.5$  mm size subhedral to euhedral clinopyroxene phenocrysts in the fine-grained plagioclase groundmass (Figure 3E). The hornblende-plagioclase andesite has been identified in diamond core (BDH1, BDH2, BDH3). It is characterized by aphanitic texture consisting of fine-grained plagioclase and pyroxene and minor hornblende (Figure 3F). The hornblende-plagioclase andesite is microscopically characterized by ophitic texture of  $<1$  mm plagioclase with minor hornblende and clinopyroxene (Figure 3G). The outcrops of the plagioclase-phyric andesite and its autobreccia are found at the northwest of Khao Moei Choi (Figure 3H). They show porphyritic texture with mainly plagioclase phenocrysts. The plagioclase-phyric andesite is characterized by porphyritic texture with plagioclase and clinopyroxene phenocrysts in the acicular plagioclase groundmass (Figure 3I).

## 2.2 Intermediate-mafic breccia (Unit 2)

The intermediate-mafic breccia unit is mainly distributed at the south of the Khao Moei Choi and north of Khao Sam Sip

extending to the north of Khao Thung Plueai area (Figure 2). It consists of polymictic andesitic sandstone and polymictic andesitic breccia (Figure 3J). This unit strikes NW-SE and dip  $50^\circ$  to the southwest. Quartz veins in width up to 10 cm, are commonly found in this unit. Under microscope, the polymictic breccia is matrix supported and it is coarse sandy to silty matrix consisting of 1 to 2 mm feldspar, lithic fragments and minor devitrified glasses (Figure 3K). The andesitic clasts show dominant plagioclase and clinopyroxene phenocrysts. Some of the andesite clasts show glassy flame-like shapes or fiamme and vesicle filled up with secondary quartz. Moreover, minor gabbroic clasts are also present, and they show phaneritic texture consisting mainly of orthopyroxene and clinopyroxene.

## 2.3 Volcanogenic-sedimentary rocks (Unit 3)

The unit of volcanogenic-sedimentary rocks is mainly distributed in the southwest of Khao Sam Sip and extends to Khao Thung Plueai (Figure 2). This unit consists of crystal-lithic sandstone, mudstone, and polymictic conglomerate. It strikes NW-SE and dip  $60^\circ$  to the southwest. Crystal-lithic sandstone crops out in the valley of Khao Sam Sip as massive grayish green sandstone and siltstone interbedded with laminated greenish gray mudstone (Figure 3L) while polymictic conglomerate exposes in southwest of the Khao Sam Sip (Figure 3M). The polymictic conglomerate consists of sub-rounded to rounded clasts of basaltic rock, granite, mudstone, and quartz pebble. Majority of the clasts are ranged from 5 to 20 cm in size. The polymictic conglomerate is matrix-supported with matrix consisting of rock fragments of fine- to coarse-grained sand particles and crystals of quartz, K-feldspar, plagioclase and clinopyroxene. Under microscope, the lithic-crystal sandstone composes mainly of crystal fragments such as plagioclase and K-feldspar and rock fragments (Figure 3N). The grain size ranges from fine- to medium-grained sand

with gradation. The silty and mudstone layers generally consist of mud and very fine-grained crystal fragments. The polymictic

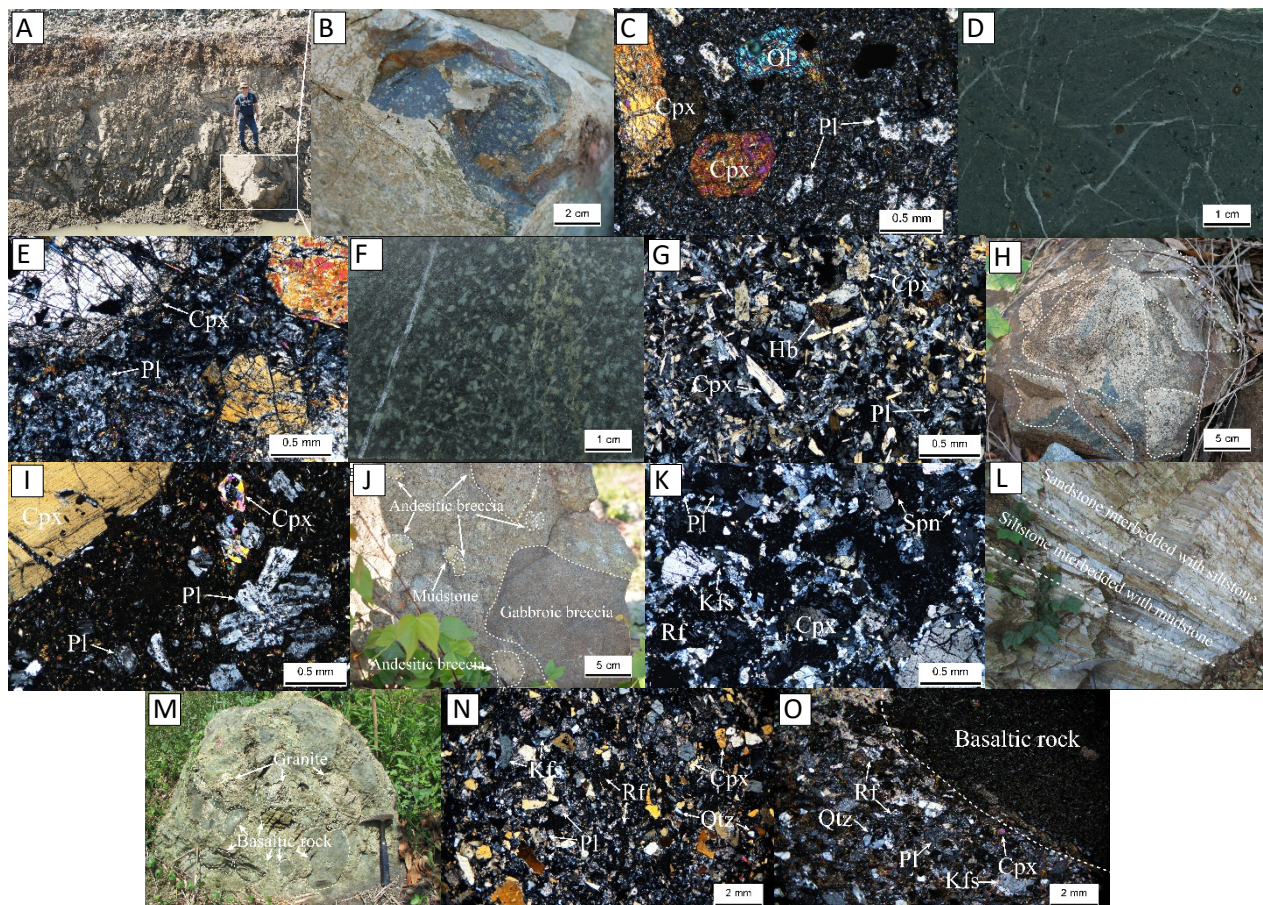


**Figure 3.** Characteristics of the volcanic units in the Khao Sam Sip area. **A)** Exposure showing the olivine-pyroxene-phyric basalt and the pyroxene-phyric basalt on the pit wall of quarry. **B)** Sample from the outcrop of pyroxene-phyric basalt showing pyroxene phenocrysts. **C)** Photomicrograph of olivine-pyroxene-phyric basalt showing groundmass consisting of plagioclase with olivine and clinopyroxene phenocrysts. **D)** Photograph of hand specimen of pyroxene-phyric basalt showing pyroxene phenocrysts (black spots). **E)** Photomicrograph of pyroxene-phyric basalt showing groundmass consisting of plagioclase and clinopyroxene phenocrysts. **F)** Hand specimen showing porphyritic texture of hornblende-plagioclase andesite. **G)** Photomicrograph of hornblende-plagioclase andesite showing plagioclase groundmass and clinopyroxene-hornblende crystals. **H)** Float rock of autobreccia of plagioclase-phyric andesite showing clast supported. **I)** Photomicrograph of plagioclase andesite showing fine-grained groundmass and phenocrysts of clinopyroxene and plagioclase. **J)** Photograph of outcrop showing dominated clasts of gabbro and andesite. **K)** Photomicrograph of matrix consisting of plagioclase, K-feldspar, clinopyroxene, sphene and rock fragments. **L)** Photograph of outcrop located at the Khao Thung Plueai showing sandstone interbedded with siltstone and mudstone. **M)** Photograph of outcrop located at the north of the Khao Sam Sip showing clasts of granite and clasts of basaltic rock. **N)** Photomicrograph of lithic-crystal sandstone consisting of plagioclase, quartz, clinopyroxene and rock fragments. **O)** Photomicrograph of polymictic conglomerate showing clast of basaltic rock in sandstone matrix which consists of quartz, plagioclase, K-feldspar, clinopyroxene and rock fragments. Abbreviation: Plagioclase = Pl, K-feldspar = Kfs, Quartz = Qtz, Rock fragments = Rf, Clinopyroxene = Cpx, Olivine = Ol, Hornblende = Hb, Sphene = Spn.

conglomerate is characterized by volcanic and non-volcanic clasts with matrix supported. The

matrix dominantly consists of medium- to coarse-grained quartz, mafic minerals and lithic

fragments as basaltic rocks and mudstone (Figure 3O).

#### **2.4. Sedimentary rocks (Unit 4)**

The sedimentary unit is the uppermost part of the sequence identified in the area. It has been observed in the south of Khao Sam Sip and extends to Khao Chan (Figure 2). This unit consists of limestone and greywacke interbedded with shale. It is inferred as Triassic age in geological map scaled to 1:250,000 of Batdambang sheet (ND 48-9) compiled by Polprasit et al. (1985). It consists of greenish-gray and greenish-black, fine- to medium-grained graywacke. The sandstone is poorly to moderately sorted, thin-bedded to massive, grade bedded, and cross-bedded in small scale. Patches of shale, interbedded shale, and limestones are also reported to be found. Limestone occurs as a tall karst-like mountain and has gray to dark gray color. It ranges in thickness from 5 to 10 cm beds with foliation by deformation.

### **3. Geochemistry**

Only coherent volcanic rocks from three volcanic rock units were chosen for geochemical study. Based on petrographic study, the least-altered samples of the coherent volcanic rocks from Unit 1 were selected for whole rock geochemical analysis which include olivine-pyroxene-plagioclase basalt, pyroxene-phyric basalt, hornblende-plagioclase andesite and plagioclase-phyric andesite. Twenty-nine volcanic rock samples were selected from drill cores and outcrop samples from Khao Sam Sip area. Whole rock major elements analysis was undertaken by measuring the fusing discs with PANalytical (Zetium) wavelength dispersive X-ray fluorescence spectrometer (WDXRF), installed at the Department of Mineral Resources (Thailand). The instrumental parameters are made up of (1) Rhodium (Rh) tube, 10 primary beam filter, 4 position collimators, 6 analyzer crystals, Vacuum seal, scintillation counter (for heavy elements) and flow proportion detectors (for light elements),

and (2) X-Ray tube is operated at 60 kV and current of up to 160 mA; at a maximum power level of 4 kW. The net (background corrected) intensities are measured and the concentrations are calculated against the calibrations derived from 3 international standard reference materials (JGb-1, GBW03101, and JB-1a). The element constituent corrections are done by the Super Q version 6.1 program.

Fourteen of the twenty-nine samples were further analyzed for trace elements and rare earth elements (REE) using Elan 6100 inductive coupled plasma mass spectrometry (ICP-MS), installed at SGS company. The ICP-MS analyses are corrected for REE-oxide interferences at the acceptable for  $\pm 10\%$  of precision range of the measurement and monitored by blank and reference solution every twenty samples.

The results of the whole rock geochemical data for the coherent volcanic rocks in the Khao Sam Sip area are listed in Tables 1 and 2.

#### **3.1 Major element data**

The four coherent volcanic groups show a range of chemical compositions from mafic to intermediate composition with alkalic affinity (Irvine and Baragar, 1971; Le Maitre et al., 1989) (Figure 4). They are plotted dominantly into trachyandesite and alkali basalt with few plots on rhyodacite, andesite and basanite fields on  $Zr/TiO_2$  vs  $Nb/Y$  diagram (Winchester and Floyd, 1977) (Figure 5). Although the samples are selected from the least-altered rocks, some samples may have been affected by secondary processes especially the hydrothermal alteration and hydrothermal mineralization presenting in the study area. Thus, to determine all selected samples in this study, the Madeisky (1996) diagram (Figure 6) is used to evaluate the effect of hydrothermal mineralization on volcanic rock samples. The diagram shows that all of rock samples from the Khao Sam Sip have molar  $(K + Na + 2Ca)/Al > 1$  considered to be unaltered rocks (Booden et al., 2010). Mg numbers ( $Mg\#$ ) were plotted against the major oxides to show the variation of  $TiO_2$ ,  $FeO_t$  and  $CaO$  between the

samples (Figure 7). The  $\text{TiO}_2$  contents are constantly low between 0.6 and 10 wt.% while  $\text{FeO}_t$  contents decrease throughout the fractionation. The bivariate plot between  $\text{CaO}$

and  $\text{Mg}^{\#}$  shows that pyroxene-phyric basalt values are slightly higher than other groups.

**Table 1.** Geochemistry of major elements (in wt.%) of least altered volcanic rocks in the Khao Sam Sip area, Sa Kaeo Province.

Sample No.	14.15-14.25	21.10-21.30	22.35-22.65	29.50-29.80	40.00-40.10	41.00-41.15	47.00-47.20	KS1-F	KS2	KS8	34.05-34.35	KS1-C	14.05-14.10	15.00-15.10	39.70-39.75
Area	BDH3	Pit	Pit	KMJ	BDH3	Pit	BDH1	BDH1	BDH1						
Rock Types	OB	OB	OB	PB	PB	HPPA	HPPA	HPPA	HPPA						
$\text{SiO}_2$	45.04	45.42	50.68	51.72	48.23	45.90	49.28	47.34	46.20	50.60	45.55	46.09	50.71	50.25	45.26
$\text{TiO}_2$	0.89	0.83	0.82	0.81	0.84	0.84	0.85	0.99	0.70	0.93	0.80	0.70	0.69	0.85	0.80
$\text{Al}_2\text{O}_3$	16.74	14.04	17.28	16.56	14.91	16.19	14.34	18.15	11.33	16.65	12.66	11.61	20.94	17.91	14.48
$\text{FeO}_t$	10.47	11.40	9.74	9.57	10.72	10.11	11.74	10.70	12.87	10.04	10.42	11.00	5.23	9.71	14.32
$\text{MnO}$	0.13	0.15	0.12	0.13	0.17	0.13	0.17	0.15	0.16	0.17	0.15	0.14	0.11	0.12	0.27
$\text{MgO}$	6.61	9.76	5.78	5.82	7.28	6.63	7.90	6.28	10.76	5.07	10.50	10.60	5.05	5.04	9.32
$\text{CaO}$	11.19	10.82	6.49	6.68	10.59	12.66	8.21	6.90	11.38	8.57	13.50	12.47	6.21	6.36	6.81
$\text{Na}_2\text{O}$	1.59	0.93	3.56	4.54	2.68	1.14	2.74	2.90	1.21	2.51	1.07	1.34	3.96	3.91	2.22
$\text{K}_2\text{O}$	1.98	2.55	2.44	1.29	0.92	2.52	1.53	2.36	1.41	2.21	1.59	1.21	3.00	2.24	1.50
$\text{P}_2\text{O}_5$	0.43	0.30	0.22	0.24	0.29	0.40	0.27	0.34	0.25	0.33	0.28	0.26	0.26	0.26	0.19
$\text{LOI}$	4.28	3.18	2.11	2.01	2.69	2.93	2.26	3.33	3.43	2.59	2.86	4.13	3.29	2.62	3.96
<b>Sum</b>	99.35	99.38	99.25	99.36	99.31	99.44	99.28	99.43	99.69	99.67	99.40	99.54	99.43	99.26	99.13
$\text{Mg}^{\#}$	38.71	46.13	37.26	37.82	40.45	39.60	40.21	37.00	45.53	33.52	50.19	49.08	49.13	34.16	39.42

Abbreviation: BDH1 = Bo Nang Ching Drill Hole 1, BDH2 = Bo Nang Ching Drill Hole 2, BDH3 = Bo Nang Ching Drill Hole 3, KMJ = Khao Moei Joi, OB = Olivine-pyroxene-plagioclase basalt, PB = Pyroxene-phyric basalt, HPPA = Hornblende-plagioclase andesite, PPA = Plagioclase-phyric andesite.

**Table 1 (Continued).**

Sample No.	41.45-41.55	19.0-19.15	51.25-51.45	51.85-52.0	53.65-53.75	45.20-45.40	8.5-8.65	48.50-48.70	29.35-29.40	38.60-38.65	24.30-24.45	25.15-25.30	42.00-42.15	25-13
Area	BDH1	BDH2	BDH2	BDH2	BDH2	BDH2	BDH3	BDH3	BDH1	BDH1	BDH2	BDH2	BDH2	KMJ
Rock Types	HPPA	HPPA	HPPA	HPPA	HPPA	HPPA	HPPA	HPPA	PPA	PPA	PPA	PPA	PPA	PPA
$\text{SiO}_2$	51.48	50.82	45.29	45.58	46.55	47.84	44.26	49.49	44.95	46.86	45.66	46.38	50.69	46.68
$\text{TiO}_2$	0.88	0.69	0.89	0.76	0.81	0.92	0.91	0.99	0.81	0.77	0.76	0.81	0.90	0.97
$\text{Al}_2\text{O}_3$	15.36	15.26	15.89	13.36	13.27	16.35	17.13	16.12	16.53	14.31	15.21	17.81	15.36	15.81
$\text{FeO}_t$	9.22	8.00	12.30	10.51	11.71	10.81	10.78	10.15	13.61	11.00	10.46	10.01	10.55	12.28
$\text{MnO}$	0.18	0.14	0.18	0.20	0.21	0.20	0.14	0.13	0.17	0.18	0.20	0.16	0.17	0.17
$\text{MgO}$	7.88	4.08	7.94	7.64	9.73	5.84	6.27	6.75	7.18	8.87	8.20	6.25	5.64	4.81
$\text{CaO}$	6.21	8.28	7.83	15.35	11.49	7.62	11.36	8.69	7.01	8.91	9.52	7.37	7.08	13.74
$\text{Na}_2\text{O}$	4.17	4.88	2.04	0.79	0.95	3.53	1.93	3.86	2.33	2.80	1.93	2.27	4.38	1.98
$\text{K}_2\text{O}$	1.50	0.40	2.28	0.87	1.86	1.80	1.81	0.41	2.29	1.53	2.82	3.15	1.12	0.92
$\text{P}_2\text{O}_5$	0.37	0.82	0.32	0.20	0.20	0.41	0.45	0.26	0.24	0.30	0.34	0.45	0.26	0.5
$\text{LOI}$	2.15	6.13	4.56	4.19	2.72	4.07	4.35	2.56	4.12	3.72	4.34	4.75	2.84	1.62

<b>Sum</b>	99.40	99.49	99.50	99.44	99.48	99.38	99.38	99.42	99.24	99.25	99.44	99.41	98.99	99.48
<b>Mg#</b>	46.11	33.77	39.21	42.10	45.39	36.76	35.07	39.92	34.54	44.63	43.96	38.42	34.82	28.13

Abbreviation: BDH1 = Bo Nang Ching Drill Hole 1, BDH2 = Bo Nang Ching Drill Hole 2, BDH3 = Bo Nang Ching Drill Hole 3, KMJ = Khao Moei Joi, OB = Olivine-pyroxene-plagioclase basalt, PB = Pyroxene-phyric basalt, HPPA = Hornblende-plagioclase andesite, PPA = Plagioclase-phyric andesite.

**Table 2.** Trace elements and REE compositions (in ppm) determined by ICP-MS analysis of least altered volcanic rocks from the Khao Sam Sip Area, Sa Kaeo Province.

Sample No.	22.35-22.65	KS1-F	KS2	KS8	KS1-C	14.05-14.10	19.00-19.15	45.20-45.40	51.85-52.00	8.50-8.65	48.50-48.70	24.30-24.45	42.00-42.15	25-13
Area	BDH3	Pit	Pit	KMJ	Pit	BDH1	BDH2	BDH2	BDH2	BDH3	BDH3	BDH2	BDH2	KMJ
Rock Types	OB	OB	OB	OB	PB	HPPA	HPPA	HPPA	HPPA	HPPA	HPPA	PPA	PPA	PPA
<b>Ba</b>	49.90	4.00	43.70	25.70	17.30	17.50	228.00	93.60	135.00	55.60	23.30	27.60	44.20	10.10
<b>Cu</b>	15.00	5.00	9.00	6.00	21.00	8.00	8.00	9.00	9.00	9.00	21.00	15.00	14.00	7.00
<b>Ni</b>	8.00	6.00	5.00	6.00	6.00	13.00	14.00	13.00	8.00	11.00	12.00	11.00	18.00	7.00
<b>Sr</b>	15.20	4.90	19.50	10.50	9.50	9.30	38.20	20.30	25.30	17.90	13.80	8.50	12.00	7.70
<b>Zn</b>	65.00	138.00	352.00	39.00	84.00	66.00	59.00	53.00	39.00	88.00	53.00	49.00	85.00	43.00
<b>Ce</b>	83.00	35.10	265.00	159.00	45.30	285.00	132.00	162.00	148.00	84.80	150.00	58.60	78.10	78.10
<b>Dy</b>	7.44	2.89	27.50	21.20	10.10	13.20	6.73	11.90	18.20	7.12	10.30	13.50	15.20	14.00
<b>Er</b>	3.81	1.43	14.10	11.30	5.73	7.03	3.49	6.82	11.00	4.36	6.12	9.08	10.30	8.55
<b>Eu</b>	0.27	0.05	0.68	0.41	0.08	0.32	0.57	0.34	0.39	0.22	0.20	0.10	0.12	0.10
<b>Gd</b>	6.38	2.29	28.80	20.30	7.10	15.30	7.31	11.30	13.90	5.11	6.85	8.76	10.50	10.40
<b>Hf</b>	4.00	3.00	10.00	6.00	4.00	15.00	11.00	8.00	9.00	5.00	8.00	12.00	17.00	6.00
<b>Ho</b>	1.45	0.51	5.14	3.95	1.93	2.46	1.32	2.42	3.79	1.45	2.13	2.96	3.27	2.85
<b>La</b>	37.60	15.50	130.00	93.00	19.20	91.00	45.70	76.30	63.10	21.70	48.50	14.10	31.50	36.90
<b>Lu</b>	0.64	0.37	2.35	1.85	1.18	1.14	0.64	1.13	1.88	0.76	1.06	1.76	2.04	1.57
<b>Nb</b>	33.00	121.00	136.00	60.00	58.00	76.00	43.00	56.00	54.00	57.00	65.00	63.00	72.00	59.00
<b>Nd</b>	31.50	13.10	154.00	108.00	19.90	84.40	42.10	60.80	55.50	18.60	34.10	17.10	32.30	31.60
<b>Pb</b>	68.00	93.00	207.00	150.00	104.00	306.00	176.00	130.00	149.00	124.00	34.00	348.00	58.00	127.00
<b>Pr</b>	9.22	3.91	41.10	29.00	5.50	24.10	12.00	18.20	16.00	5.47	10.30	4.42	8.79	9.25
<b>Rb</b>	734.00	1310.00	805.00	811.00	972.00	284.00	666.00	629.00	979.00	713.00	602.00	904.00	500.00	564.00
<b>Sb</b>	0.70	0.50	0.60	0.40	0.40	0.90	0.50	0.50	0.90	1.70	1.30	0.30	2.10	0.60
<b>Sm</b>	7.60	3.00	36.70	26.60	7.40	19.50	9.10	13.40	13.80	5.10	7.30	6.50	10.20	9.40
<b>Sn</b>	100.00	365.00	65.00	97.00	324.00	103.00	59.00	89.00	86.00	131.00	117.00	158.00	294.00	138.00
<b>Ta</b>	12.60	60.50	20.40	18.00	26.50	16.30	8.70	12.00	13.60	21.20	15.50	26.20	26.90	17.80
<b>Tb</b>	1.24	0.46	4.74	3.58	1.64	2.37	1.19	2.01	2.78	1.07	1.54	2.02	2.21	2.13
<b>Th</b>	56.20	25.60	80.80	70.10	30.40	189.00	141.00	143.00	86.50	57.00	103.00	58.10	77.50	59.60
<b>Tm</b>	0.59	0.27	2.34	1.82	1.00	1.09	0.58	1.05	1.80	0.73	0.99	1.53	1.71	1.42
<b>U</b>	14.70	5.74	29.10	20.40	7.58	23.20	32.50	24.80	15.50	28.50	13.40	28.90	11.10	13.40
<b>Y</b>	43.50	17.20	153.00	116.00	61.70	72.70	32.40	73.80	125.00	45.00	67.20	96.50	95.90	87.00
<b>Yb</b>	4.00	2.30	16.10	12.50	7.70	7.40	4.10	7.20	12.50	5.10	6.80	10.80	12.90	9.70
<b>Zr</b>	106.00	49.20	233.00	120.00	49.00	328.00	299.00	191.00	247.00	89.10	211.00	243.00	311.00	109.00
<b>Zr/Y</b>	2.44	2.86	1.52	1.03	0.79	4.51	9.23	2.59	1.98	1.98	3.14	2.52	3.24	1.25
<b>Ti/Y</b>	113.54	345.35	27.23	48.00	67.52	56.97	126.91	74.32	36.20	121.48	88.30	46.90	56.06	66.76
<b>[La/Sm]n</b>	3.19	3.34	2.29	2.26	1.67	3.01	3.24	3.68	2.95	2.75	4.29	1.40	1.99	2.53
<b>[Sm/Yb]n</b>	2.11	1.45	2.53	2.36	1.07	2.93	2.47	2.07	1.23	1.11	1.19	0.67	0.88	1.08

Abbreviation: BDH1 = Bo Nang Ching Drill Hole 1, BDH2 = Bo Nang Ching Drill Hole 2, BDH3 = Bo Nang Ching Drill Hole 3, KMJ = Khao Moei Joi, OB = Olivine-pyroxene-plagioclase basalt, PB = Pyroxene-phyric basalt, HPPA = Hornblende-plagioclase andesite, PPA = Plagioclase-phyric andesite.

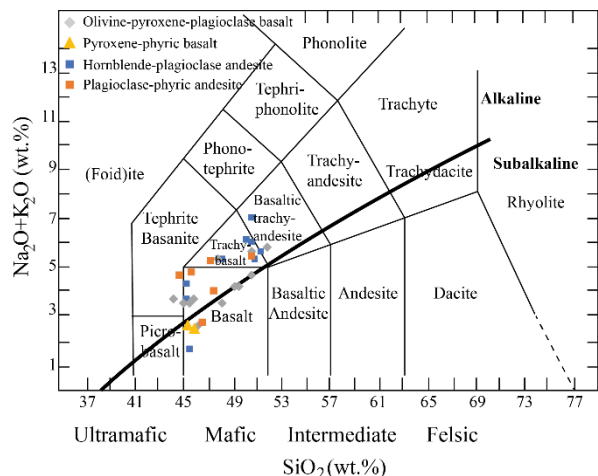


**Figure 4.**  $\text{Na}_2\text{O} + \text{K}_2\text{O}$  vs  $\text{SiO}_2$  discrimination diagram by Irvine and Baragar (1971); Le Maitre et al. (1989).

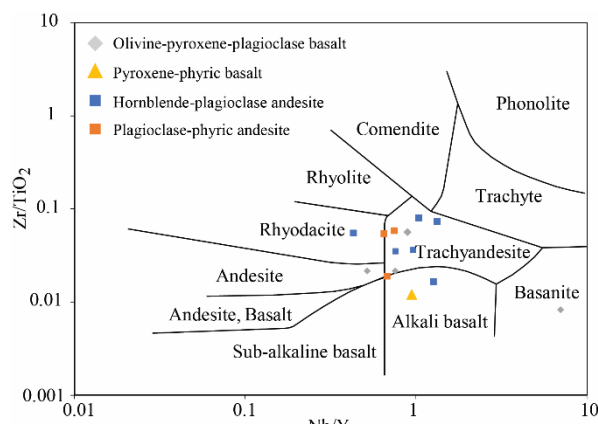


**Figure 5.**  $\text{Nb}/\text{Y}$  and  $\text{Zr}/\text{TiO}_2$  discrimination diagram by Winchester and Floyd (1977).

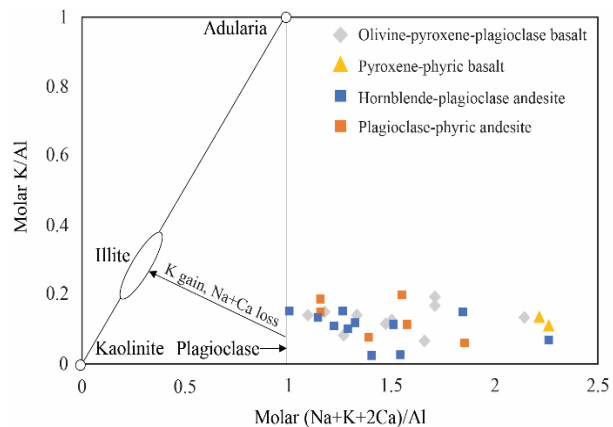


**Figure 6.** Molar  $\text{K}/\text{Al}$  vs. molar  $(\text{K} + \text{Na} + 2\text{Ca})/\text{Al}$  (Madeisky, 1996; Booden et al., 2010). In this diagram, the alteration minerals kaolinite, illite and adularia plot on a line of slope 1. Unaltered basaltic to andesitic volcanic rocks typically have molar  $(\text{K} + \text{Na} + 2\text{Ca})/\text{Al}$  values  $> 1$ . Potassium metasomatism leads to decreasing molar  $(\text{K} + \text{Na} + 2\text{Ca})/\text{Al}$  and increasing molar  $\text{K}/\text{Al}$  values. Most of the Khaosam Sip rocks have molar  $(\text{K} = \text{Na} + 2\text{Ca})/\text{Al} > 1$  and considered to be the least altered rocks.

### 3.2 Trace element and REE data

Trace elements and REE plots against Mg# in bivariate diagrams show that the transition elements such as Ni and large ion lithophile elements (LILE) including Sr scatter widely reflecting their tendency to be mobilized due to hydrothermal processes and/or low metamorphism (Frey et al., 1974; Floyd, 1977; Hellman and Henderson, 1977; Humphris et al., 1978; Whitford et al., 1988) (Figure 8A and B). Significantly, hornblende-plagioclase andesite has higher Sr concentrations than the other groups. Moreover, high fields strength elements (HFSE) such as Nb, Zr and Y are relatively immobile during hydrothermal processes (Winchester and Floyd, 1977; MacLean and Barrett, 1993; Rollinson, 1993). The bivariate plots of HSFE against Mg# show a slight difference in each rock type. The hornblende-plagioclase andesite and plagioclase-phyric andesite have constant Nb concentrations while the olivine-pyroxene-plagioclase basalt shows scattering Nb concentrations (Figure 8C). There

is a positive trend between Zr against Mg# values in all rock types except pyroxene-phyric basalt (Figure 8D). The bivariate plot of Y against Mg# shows that the first sub-group of olivine-pyroxene-plagioclase basalt has the lowest concentrations of Y while the second sub-group has the highest concentrations of Y (Figure 8E). Plagioclase-phyric andesite has consistent Y concentrations around 80 ppm, whereas hornblende-plagioclase andesite has varied Y concentrations ranging from 20 to 120 ppm.

The chondrite normalized REE patterns using values of Sun and McDonough (1989) confirm that at least four separate magmatic suites are present at the Khao Sam Sip area (Figure 9). All samples have abundant REE which represent the highly evolved magma with strong negative Eu anomalies and flat slope for heavy rare-earth elements (HREE). The olivine-pyroxene-plagioclase basalt and hornblende-plagioclase andesite have a similar pattern of higher light rare-earth elements (LREE) relative

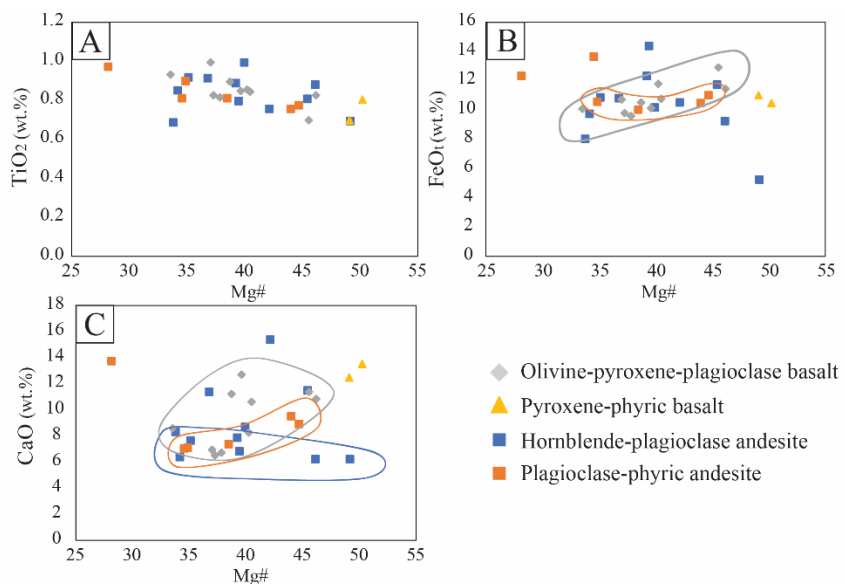


**Figure 7.** Major element bivariate diagram plotted against Mg# for the volcanic rocks from the Khao Sam Sip area. A)  $\text{TiO}_2$  vs Mg# number showing an increase  $\text{TiO}_2$  with decrease Mg#, B)  $\text{FeO}_t$  vs Mg# showing a slightly positive trend to more mafic composition, C)  $\text{CaO}$  vs Mg# showing the different fields among the volcanic groups.

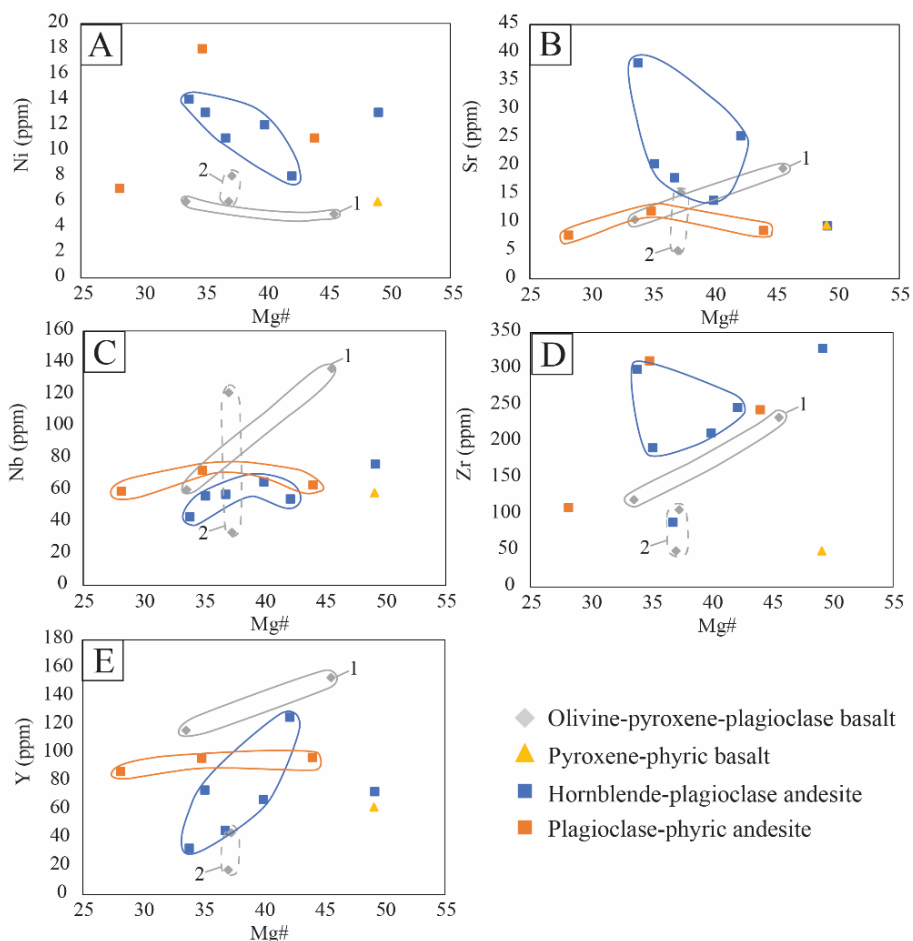


**Figure 8.** Trace element bivariate diagram plotted against Mg# for the volcanic rocks from the Khao Sam Sip area. A) Ni vs Mg#, B) Sr vs Mg#, C) Nb vs Mg#, D) Zr vs Mg#, and E) Y vs Mg#.

to HREE than that of pyroxene-phyric basalt and plagioclase-phyric andesite. The olivine-pyroxene-plagioclase basalt has high LREE with chondrite-normalized La/Sm = 2.26-3.34 and Sm/Yb = 1.45-2.53. The pyroxene-phyric basalt has is slightly high in LREE with chondrite-normalized La/Sm = 1.67 and Sm/Yb = 1.07. The hornblende-plagioclase andesite has increasing values in LREE with chondrite-normalized La/Sm and Sm/Yb for 2.75-4.29 and 1.11-2.93 respectively. The plagioclase-phyric andesite is slightly high in LREE with chondrite-normalized La/Sm for 1.40-2.53 and Sm/Yb for 0.67-1.08.

The N-MORB normalized (Sun and McDonough, 1989) multi-element plot (Figure 10) reveals distinct negative anomalies in Ba, Sr, Eu and Ti and enrichments of Rb, Th, U, Ta and especially Pb relative to other elements compared to MORB. The olivine-pyroxene-plagioclase basalt and hornblende plagioclase andesite are higher in their incompatible element contents in comparison to the pyroxene phyric basalt and plagioclase-phyric andesite. The olivine-pyroxene-plagioclase basalt and hornblende-plagioclase andesite have the similar N-MORB normalized multi-element pattern to the alkali rock from Valle del Leone, Etna Mount which is related to the magma in subduction zone (Armienti et al., 2004). The pyroxene-phyric basalt and plagioclase-phyric andesite have the similar N-MORB normalized multi-element pattern to the alkali rock from Coriolis Trough basin, Vanuatu (Sun et al., 2003).

### 3.3 Implication for magmatic affinity and tectonic setting of formation

Several selected tectono-magmatic discrimination diagrams are used to analyze the tectonic setting of the coherent volcanics of the Khao Sam Sip area. The diagrams used to discriminate tectonic environments of the studied rocks include MnO-TiO<sub>2</sub>-P<sub>2</sub>O<sub>5</sub> (Mullen, 1983), TiO<sub>2</sub> vs Zr (Pearce and Cann, 1973), and Zr/Y vs Ti/Y (Pearce and Gale, 1977) diagrams. All the volcanic groups

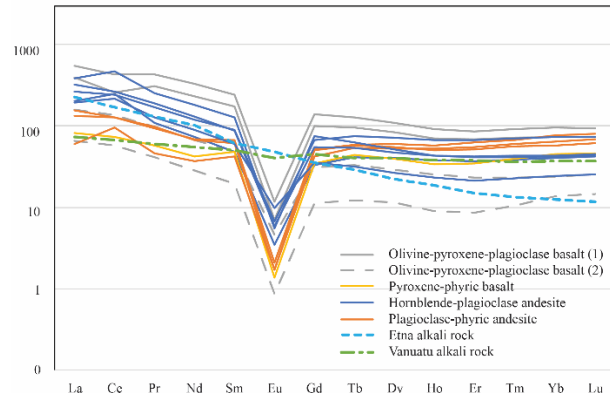


**Figure 9.** Chondrite-normalized REE patterns of the representative volcanic rocks in the Khao Sam Sip plotted using chondrite normalizing values of Sun and McDonough (1989).

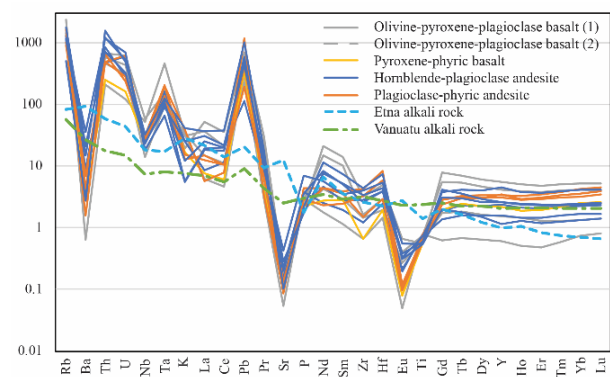


**Figure 10.** N-MORB normalized trace elements patterns for the volcanic rocks in the Khao Sam Sip area. The N-MORB composition is taken from Sun and McDonough (1989).

appear to be island arc basalt, with calc-alkaline characters, as shown in the MnO-TiO<sub>2</sub>-P<sub>2</sub>O<sub>5</sub> plots (Figure 11A). Their plots are corresponded to the fields of volcanic arc basalt in the TiO<sub>2</sub> vs Zr (Figure 11B) and plate margin field in the Zr/Y vs Ti/Y (Figure 11C) diagrams.

### 4. Mineralization

At Khao Sam Sip, mineralization occurs as veins/veinlets hosted in volcanic rocks mainly in Unit 1 (coherent rocks). Based on crosscutting relationships, mineral assemblages and textural features, at least 3 stages of mineralizations (veining) have been identified namely, 1) pre-copper, 2) copper stage, and post copper stage (Table 3).

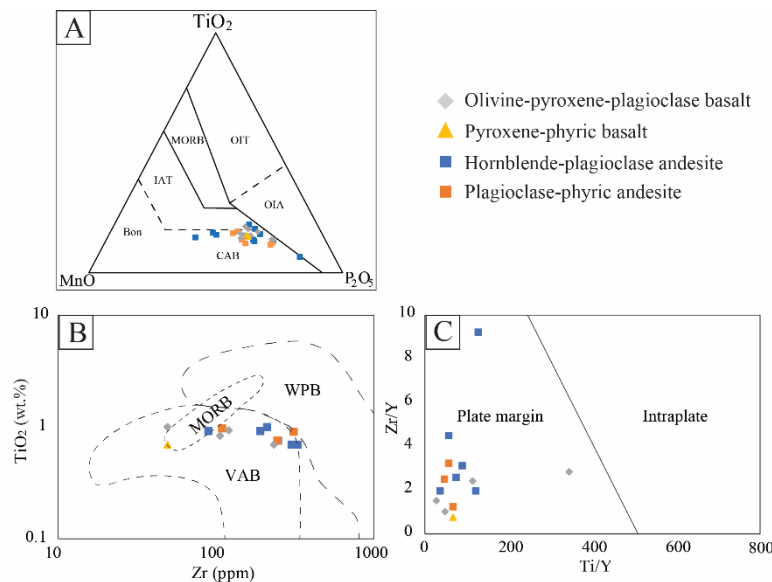


**Figure 11.** Tectonic discrimination diagrams for volcanic rocks from the Khao Sam Sip area: A) Plot of  $\text{MnO}^*10\text{-TiO}_2\text{-P}_2\text{O}_5^*10$  (Mullen, 1983) showing the field for MORB = mid ocean ridge basalt; OIT = ocean-island tholeiite or sea mount tholeiite; OIA = ocean-island alkali basalt or seamount alkali basalt; CAB = island-arc calc alkaline basalt; IAT = island-arc tholeiite; Bon = boninite. Note that for the volcanic rocks plot in the island-arc calc alkaline basalt field, B) Plot of  $\text{TiO}_2$  against  $\text{Zr}$  showing the field for MORB = mid ocean ridge basalt; VAB = volcanic arc basalt; WPB = within-plate basalt. Note that for the volcanic rocks plot in the volcanic arc basalt field, C) Plot of  $\text{Zr/Y}$  against  $\text{Ti/Y}$ . Note that for the volcanic rocks plot in the plate margin field.

**Table 3.** Mineralization stages and the paragenesis of the Khao Sam Sip area.

Minerals	Stage 1	Stage 2	Stage 3	Stage 4
Quartz	---	—	---	—
Calcite		----		---
Pyrite	—	---		
Chalcopyrite		—		
Sphalerite		---		
Epidote			—	
Chlorite			—	

Stage 1: pre-copper mineralization is characterized by quartz-pyrite veins/veinlets (Figure 12A and B). Stage 2: copper (-Au) mineralization is characterized by quartz-chalcopyrite-pyrite ( $\pm$ sphalerite-gold) veins/veinlets. Stage 2 veins/veinlets appear to crosscut Stage 1 veins/veinlets observed both in drill core samples and thin sections under

microscope (Figure 12A). Ore minerals in this stage are dominated by chalcopyrite as major sulfide with minor pyrite and sphalerite. Pyrite tends to occur peripheral to the veins/veinlets and closely associated with subhedral to euhedral quartz followed by chalcopyrite toward the center of veins (Figure 12C). Chalcopyrite is closely associated with carbonate minerals (mainly calcite) (Figure 12D). No gold has been identified during this study, but it has been reported in assay data for ppb level (Department of mineral and resources, 2011). Stage 3: quartz  $\pm$  epidote  $\pm$  chlorite veins/veinlets comprise quartz and epidote or chlorite, and Stage 4: quartz  $\pm$  carbonate veins/veinlets are mainly composed of quartz and/or carbonate. No sulfides have been identified in the Stage 3 and Stage 4.

## 5. Discussion

### 5.1 Magmatic suites at the Khao Sam Sip

Based on field observation and petrographic characteristics, the volcanic rocks

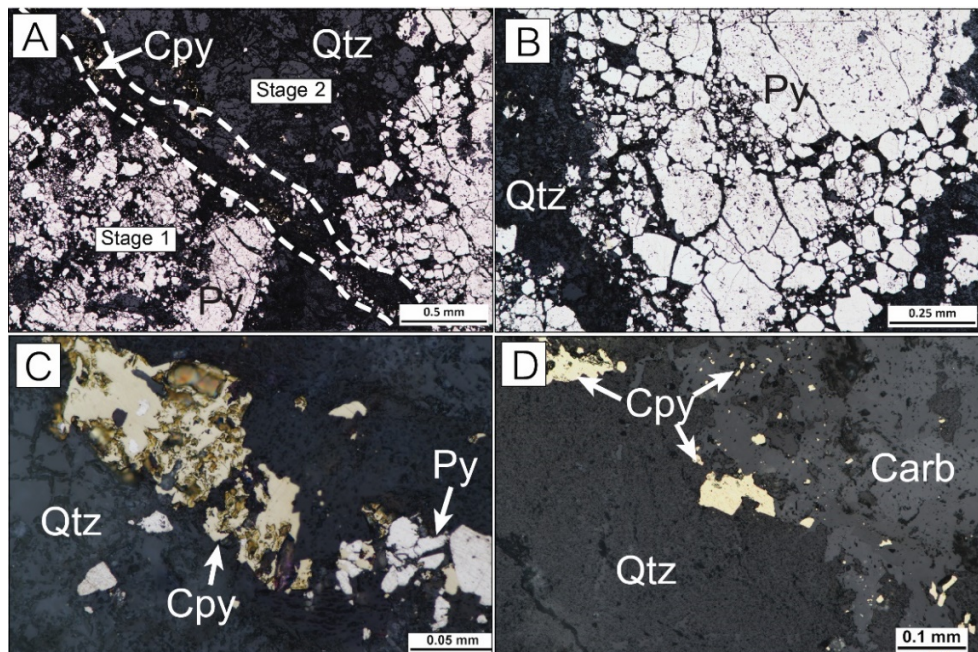


**Figure 12.** Characteristics of mineralization stages of the Khao Sam Sip area. **A)** Photomicrograph of mineralization Stage 1 vein and Stage 2 showing crosscutting relationship. **B)** Photomicrograph of stage 1 showing subhedral pyrite aggregate in quartz vein. **C)** Photomicrograph of stage 2 showing pyrite and chalcopyrite assemblage associated with quartz vein. **D)** Photomicrograph showing chalcopyrite is closely associated with carbonate minerals. Abbreviation: Quartz = Qtz, Chalcopyrite = Cpy, Pyrite = Py, Carbonate = Carb.

at the Khao Sam Sip are classified into three main units: a) Coherent volcanic rocks, b) Intermediate-mafic breccia and c) Volcanogenic sedimentary rock units. They are constituted by mafic to intermediate volcanic and volcaniclastic rocks. In the coherent volcanic rock sequence, there are four rock types: 1) Olivine-pyroxene-plagioclase basalt, 2) Pyroxene-phyric basalt, 3) Hornblende-plagioclase andesite and 4) Plagioclase-phyric andesite. All of the rock types in this unit occur as lava flows with different phenocryst assemblages, except for the hornblende-plagioclase andesite showing ophitic texture which is typical of dyke-like rocks.

Based on major and trace elements and REE of the coherent volcanic rocks at the Khao Sam Sip area, majority of the rocks show alkaline affinity based on high  $\text{Na}_2\text{O} + \text{K}_2\text{O}$  contents, and the rocks are dominantly ranged in trachyandesite, alkali basalt and basanite in chemical compositions. 1) Olivine-pyroxene-plagioclase basalt is characterized by low Ti, Ni and Zr, with

moderate Sr and Nb. 2) Pyroxene-phyric basalt is characterized by low Ti, Ni, Sr, Nb, Zr and Y; however, only one samples of the pyroxene-phyric basalt has been examined in this study. To give more precise characteristic of the pyroxene-phyric basalt, more samples need to be analyzed. 3) Hornblende-plagioclase andesite is characterized by high Ni, Sr and Zr and low Nb and Y. 4) Plagioclase-phyric andesite is characterized by low Ti with various Ni and Zr but constant Nb and Y which are greater than the hornblende-plagioclase andesite while the Sr concentrations are as same as the olivine-pyroxene-plagioclase basalt.

## 5.2 Magma sources

The trace elements and REE have been used to establish petrochemical characteristic and deduce magma source of the coherent volcanic rocks at Khao Sam Sip. The coherent volcanic rocks are divided into two evolved comagmatic sources, as evidenced by narrow ranges of least-mobile element ratios (e.g.  $\text{La}/\text{Sm}$ ,  $\text{Sm}/\text{Yb}$  and  $\text{La}/\text{Yb}$ ). One out of two

magmatic sources show more enrichment of LREE relative to HREE than the other one. In addition, a comparison with those modern analogs has been carried out. As the result, the olivine-pyroxene-plagioclase basalt and the hornblende-plagioclase andesite are similar to the alkali rock from Valle del Leone, Etna Mount (Armienti et al., 2004) while the pyroxene-phyric basalt and the plagioclase-phyric andesite are similar to the alkali rock from Coriolis Trough basin, Vanuatu (Sun et al., 2003).

### 5.3 Tectonic setting and magmatic affinity

The coherent volcanic rock units at the Khao Sam Sip area are chemically characterized by enrichment in HFSE such as Th, U, Ta and Pb and alkalic affinity with subduction-related magmatic setting. Such enrichment in some HFSE may suggest crustal contamination for the evolved magma. In addition, all the analyzed rocks show distinct negative Eu anomalies in REE patterns, and this may indicate that the rocks were formed from highly fractionated magma.

Timing of magmatism of these volcanic rocks at Khao Sam Sip is indicated to be Early Triassic by zircon U-Pb age of  $246 \pm 3$  Ma for volcanic breccia collected from Unit 2 (Salam et al., 2012). A similar age ( $247 \pm 6$  Ma) is also obtained from volcaniclastic rocks at the French Mine area about 30 km to west of the Khao Sam Sip area (Khin Zaw et al., 2009). In general, major volcanism period of the LFB is confined to Late Permian-Early Triassic (Jungyusuk and Khositanont, 1992; Intasopa and Dunn, 1994; Salam et al., 2014) and dominated by subalkaline rocks (tholeiite and calc-alkaline affinities). However, the volcanic rocks at Khao Sam Sip are identified to be Early Triassic alkaline series, and this is very unique characteristic for the volcanic rocks of the LFB.

### 5.4 Mineralization

Based on mineral assemblages and textural features, the mineralization occurring at Khao Sam Sip can be a skarn system (distal skarn?) similar to the French Mine skarn

(Khin Zaw et al., 2009). At French Mine, the skarn mineralization is likely to be associated with Late Triassic ( $203 \pm 6$  Ma) diorite that has been responsible for gold skarn mineralization (Khin Zaw et al., 2009). Alternatively, it can be an epithermal system as occurrence of copper-rich epithermal deposit was reported in NW of Cambodia, at extensional zone of LFB (e.g. Kousa Cu deposit; Manaka et al., 2014).

On the basis of available diamond drill holes at Khao Sam Sip, the copper mineralization occurrence is spatially confined to the coherent volcanic unit (Unit 1). However, it cannot be ruled out that the copper mineralization is hosted in other units. Considering in Unit 1, the mineralization is weakly developed which may be due to poorly developed structures (e.g. fault) together with less suitable lithology (e.g. coherent rocks). In contrast, the Chatree epithermal deposit is also hosted in volcanics of similar ages (Salam et al., 2014).

### 6. Conclusion

The results of field investigation, petrography and geochemistry of the volcanic rocks in the Khao Sam Sip area, Sa Kaeo province can draw conclusions below.

- 1) The volcanic rocks in this study area are coherent volcanic and volcanic clastic rocks and they can be divided into three main units namely, 1 ) Coherent volcanics unit, 2 ) Intermediate-mafic breccia unit, and 3 ) Volcanogenic-sedimentary unit.
- 2) The geochemical data of the coherent volcanics unit show compositional ranges from basalt to andesite with alkalic affinity.
- 3) The trace and REE chemical data of the volcanic rocks are characterized by enrichment in HFSE (e.g. Th, U, Ta, Pb) and distinct negative Eu anomalies, indicating that their source was highly fractionated magma with crustal contamination formed in volcanic arc.

- 4) The magmatism responsible for the formation of volcanic rocks in Khao Sam Sip area is chronologically indicated to be a part of LFB, but has unique characteristics of alkaline affinity, which is rarely found among volcanic rocks of LFB.
- 5) The coherent volcanic rocks (Unit 1) host Cu±Au veins/veinlets, which can be classified as skarn or epithermal deposit types.

### **Acknowledgement**

We would like to thank staffs at Department of Geology, Faculty of Science, Chulalongkorn University for the great support. As well as, we would like to thank to Department of Mineral Resource for providing access to the drill core samples and XRF analysis its staffs at the Rayong Division and the Head Office for the great support.

### **References**

Armienti, P., Tonarini, S., Orazio, D. M., and Innocenti, F. 2004. Genesis and evolution of Mt. Etna alkaline lavas: petrological and Sr-Nd-B isotope constraints. *Periodio di Mineralogia*, 73, 29-52.

Barr, S. M., and Macdonald, A. S., 1978. Geochemistry and Petrogenesis of Late Cenozoic Alkaline Basalts of Thailand. *Geological Society of Malaysia Bulletin*, 10, 25-52.

Barr, S. M., and Macdonald, A. S. 1987. Nan River suture zone, northern Thailand. *Geology* 15: 907-910.

Barr, S. M., Tantisukrit, C., Yaowanoiyothin, W., and Macdonald, A. S. 1990. Petrology and tectonic implications of Upper Paleozoic volcanic rocks of the Chiang Mai belt northern Thailand. *Journal of Southeast Asian Earth Science*, 4, 37-47.

Barr, S. M., Macdonald, A. S., Dunning, G. R., Ounchanum, P., and Yaowanoiyothin, W. 2000. Petrochemistry, U-Pb (zircon) age, and palaeotectonic setting of the Lampang volcanic belt, northern Thailand. *Journal of the Geological Society, London*, 157, 553-563.

Boonduen, M.A., Smith, I.E.M., Mauk, J.L., Black, P.M., 2010. Evolving volcanism at the tip of a propagating arc: the earliest High-Mg andesites in northern New Zealand. *Journal of Volcanology and Geothermal Research*, 195, 83-96.

Bunopas, S., and Vella, P., 1983. Tectonic and geologic evolution of Thailand. In: P. Nutalaya (Ed.), *Geological Society of Thailand and Geological Society of Malaysia*. Bangkok, 307-322.

Charusiri, P., Daorerk, V., Archibald, D., Hisada, K., & Ampaiwan, T., 2002. Geotectonic evolution of Thailand: A new synthesis. *Journal of the Geological Society of Thailand*, 1, 1-20.

Department of mineral resources, 2011. Accelerated Mineral Resources Exploration and Evaluation Project (AMREEP) report. Mineral Resources division, Department of Mineral Resources, Bangkok.

Floyd, P.A., 1977. Rare earth element mobility and geochemical characterization of spilitic rocks. *Nature*, 269, 134-137.

Frey, F.A., Bryan, W.B. and Thompson, G., 1974. Atlantic Ocean floor - Geochemistry and petrology of basalts from Legs 2 and 3 of the Deep-Sea Drilling Project. *J. Geophys. Res.*, 70, 5507-5527.

Hellman, PL. and Henderson, P., 1977. Are rare earth mobile during spilitization? *Nature*, 267, 38-40.

Humphris, S.E., Morrison, M.A. and Thompson, R.N., 1978. Influence of rock crystallization history upon subsequent lanthanide mobility during hydrothermal alteration of basalts. *Chem. Geol.*, 23, 125-137.

Intasopa, S., 1993. Petrology and geochronology of the volcanic rocks of the Central Thailand volcanic belt. PhD. Geology, Chulalongkorn University.

Intasopa, S., Dunn, T., 1994. Petrology and Sr-Nd isotopic systems of the basalts and rhyolites, Loei, Thailand.

Irvine, T. N., & Baragar, W. R. A. 1971. A Guide to the Chemical Classification of the Common Volcanic Rocks. *Canadian Journal of Earth Sciences*, 8(5), 523-548.

Jungyusuk, N., Khositanont, S., 1992. Volcanic rocks and associated mineralization in Thailand. In C. Piencharoen (Ed.), *Department of Mineral Resources*. Bangkok, 522-538.

Khin, Zaw, Meffre, S., Kamvong, T., Khositanont, S., Stein, H., Vasconcelos, P., and Golding, S., 2009. Geochronological and metallogenetic framework of Cu-Au skarn deposits along Loei

Fold Belt, Thailand and Lao PDR., Proceedings of the 10th biennial SGA meeting, Townsville, Australia, 17-20 August 2009, 309-311.

Khin Zaw, Meffre, S., Lai, C.K., Santosh, M., Burrett, C., Graham, I.T., Manaka, T., Salam, A., Kamvong, T., Cromie, P. W., 2014. Tectonics and metallogeny of mainland Southeast Asia- a review and contribution. *Gondwana Research*, 26, 5-30.

Kosuwan, P., J., Limtrakun, P., Boonsoong, P., and Panjasawatwong, Y. 2017. Petrography and REE Geochemical Characteristics of Felsic to Mafic Volcanic Hypabyssal Rock in Nakhon Sawan and Uthai Thani Provinces, Central Thailand. *Chiang Mai Journal Science* 44(4): 1722-1734.

Le Maitre, R.W., Bateman, P., Dudek, A., Keller, J., Lameyre Le Bas, M.J., Sabine, P.A., Schmid, R., Sorensen, H., Streckensen, A., Wooley, A.R., Zanettin, B., 1989. A classification of igneous rocks and glossary of terms. Blackwell, Oxford.

MacLean, W.H., Barrett, T.J., 1993. Lithogeochemical techniques using immobile elements. In: Hoffman, E.L., Moore, D.W. (Eds.), *Journal of Geochemical Exploration*, 48, 109-133.

Madeisky, H.E., 1996. A lithogeochemical and radiometric study of hydrothermal alteration and metal zoning at the Cinola epithermal gold deposit, Queen Charlotte Islands, British Columbia. In: Coyner, A.R., Fahey, P.I.L., (Eds.), *Geology and Ore Deposits of the American Cordillera*, 1153-1185.

Manaka, T., Zaw, K., Meffre, S., Salam, A. and Lim, Y., 2014. An overview of geological setting and ore deposits of Southern Indochina – a focus on Cambodia. *Proceedings of Sundaland Resources 2014 MGEI Annual Convention*. 17-18 November 2014, Palembang, South Sumatra, Indonesia. 103-107.

McPhie, J., Doyle, M., Allen, R. 1993. Volcanic Texture, 1-179.

Metcalfe, I., 2009. Late Palaeozoic and Mesozoic tectonic and palaeogeographical evolution of SE Asia. Geological Society, London, Special Publications, 315(1), 7-23.

Morley, C. K. 2014. The widespread occurrence of low-angle normal faults in a rift setting: Review of examples from Thailand, and implications for their origin and evolution. *Earth-Science Reviews* 133, 18-42.

Mullen, E.D., 1983. MnO/TiO<sub>2</sub>/P<sub>2</sub>O<sub>5</sub> - a minor element discrimination for basaltic rocks of oceanic environment and its implications for petrogenesis. *Earth Planet. Sci. Lett.*, 62, 53-62.

Panjasawatwong, Y., Yaowanoiyothin, W., 1993. Petrochemical study of post-Triassic basalts from the Nan Suture, northern Thailand. *Journal of Southeast Asian Earth Sciences*, 8, 147-158.

Panjasawatwong, Y., Zaw, K., Chantaraamee, S., Limtrakun, P., and Pirarai, K., 2006. Geochemistry and tectonic setting of the Central Loei volcanic rocks, Pak Chom area, Loei, northeastern Thailand. *Journal of Asian Earth Sciences*, 26, 77-90.

Pearce, J.A., Cann, J.R., 1973. Tectonic setting of basic volcanic rocks determined using trace element analyses. *Earth and Planetary Science Letters*, 19, 290-300.

Pearce, J.A. and Gale, G.H., 1977. Identification of ore-deposit environment from trace element geochemistry of associated igneous host rocks. *Geol. SOC. London, Spl. Publ.*, 7, 14-24.

Polprasit, C., Paijiprapaporn, V., Thitisawan, V., and Tansathien, W., 1985. Geologic Map of Batdambang (Sheet ND 48-9, Scale 1: 250,000), Geological Survey Division: Department of Mineral Resources. Bangkok.

Qian, X., Wang, Y., Srithai, B., Feng, Q., Zhang, Y., Zi, J.-W., and He, H., 2017. Geochronological and geochemical constraints on the intermediate-acid volcanic rocks along the Chiang Khong–Lampang–Tak igneous zone in NW Thailand and their tectonic implications. *Gondwana Research*, 45, 87-99.

Rollinson, H.R., 1993. *Using Geochemical Data: Evolution, Presentation and Interpretation*. Longman, 1-214.

Salam, A. 2013. A geological, geochemical and metallogenic study of the Chatree Epithermal Deposit, Phetchabun Province, central Thailand. Unpublished PhD. thesis, Geology, University of Tasmania.

Salam, A., Zaw, K., Meffre, S., Manaka, T., and Khositanont, S. 2012. Sukhothai and Loei belts in Eastern Thailand and Cambodia. CODES Ore Deposits of SE Asia project report (Unpublished) – Report No. 4.

Salam, A., Zaw, K., Meffre, S., McPhie, J., and Lai, C. 2014. Geochemistry and geochronology of the Chatree epithermal gold-silver deposit: Implications for the tectonic

setting of the Loei Fold Belt, central Thailand. *Gondwana Research* 26, 198-217.

Singharajwapan, S. 1994. Deformation and metamorphism of the Sukhothai fold belt, northern Thailand. PhD. University of Tasmania.

Sone, M., and Metcalfe, I., 2008. Parallel Tethyan sutures in mainland Southeast Asia: New insights for Palaeo-Tethys closure and implications for the Indosinian orogeny. *Comptes Rendus Geoscience* ,340, 166-179.

Sun, S.-S., McDonough, W.F., 1989. Chemical and isotopic systematics of oceanic basalts: implications for mantle composition and processes. In: Saunders, S., Norry, M. J. (Eds.), *Magmatism in the Ocean Basins*. Geological Society of London Special Publication, 313-345.

Sun, W., Bennett, V.C., Eggins, S.M., Arculus, R.J., Perfit, M.R., 2003. Rhenium systematics in submarine MORB and back-arc basin glasses: laser ablation ICP-MS results. *Chemical Geology*, 196, 259–281.

Whitford, D.J., Korsch, M. J., Porritt, P.M. and Craven, S.J., 1988. Rare-earth mobility around the volcanogenic polymetallic massive sulfide deposit at Que River, Tasmania, Australia. *Chem. Geol.*, 68, 105-119.

Winchester and Floyd, 1977. Geochemical discrimination of different magma series and their differentiation products using immobile elements. *Chemical Geology*, 20, 325-343.